

9-1983

Self-Refraction of Nonlinear Capillary-Gravity Waves

Partha P. Banerjee

University of Dayton, pbanerjee1@udayton.edu

Adrianus Korpel

University of Iowa

Karl E. Lonngren

University of Iowa

Follow this and additional works at: https://ecommons.udayton.edu/ece_fac_pub



Part of the [Computer Engineering Commons](#), [Electrical and Electronics Commons](#), [Electromagnetics and Photonics Commons](#), [Optics Commons](#), [Other Electrical and Computer Engineering Commons](#), and the [Systems and Communications Commons](#)

eCommons Citation

Banerjee, Partha P.; Korpel, Adrianus; and Lonngren, Karl E., "Self-Refraction of Nonlinear Capillary-Gravity Waves" (1983). *Electrical and Computer Engineering Faculty Publications*. 218.

https://ecommons.udayton.edu/ece_fac_pub/218

This Article is brought to you for free and open access by the Department of Electrical and Computer Engineering at eCommons. It has been accepted for inclusion in Electrical and Computer Engineering Faculty Publications by an authorized administrator of eCommons. For more information, please contact frice1@udayton.edu, mschlange1@udayton.edu.

Self-refraction of nonlinear capillary-gravity waves

P. P. Banerjee, A. Korpel, and K. E. Lonngren

Department of Electrical and Computer Engineering, The University of Iowa, Iowa City, Iowa 52242

(Received 14 January 1983; accepted 3 June 1983)

Self-refraction effects have been observed during the propagation of deep-water capillary-gravity waves. The observations are shown to be in qualitative agreement with the theory of self-focusing and defocusing in a cubically nonlinear medium in the presence of diffraction.

I. INTRODUCTION

This paper is the second report on a series of experiments devoted to investigating the effect of quadratic and cubic nonlinearities on wave propagation in a dispersive medium. In an earlier paper¹ we reported on subharmonic generation caused by the quadratic nonlinearity, and showed the observations to be in semiquantitative agreement with theory. The present paper deals with the cubic nonlinearity.

The effect of a cubic nonlinearity on wave propagation, both continuous and pulsed, has been theoretically studied over the past few years.² In particular, the phenomenon of self-focusing has been observed and analyzed in the field of nonlinear optics, during the propagation of intense laser beams. In this case the induced polarization is nonlinear, giving rise to a dielectric constant, and hence refractive index, that increases as the square of the field amplitude. For an input profile that monotonically decreases away from the axis, the refractive index is therefore a maximum on the propagation axis. This triggers a cumulative process whereby "rays" that are initially parallel to the propagation axis bend towards it. This self-focusing action causes a reduction in the beam waist size.

In this paper we report on a simple experiment using deep-water capillary-gravity waves for which both self-focusing and self-defocusing are observed, depending on the frequency of operation. In the capillary wave regime the phase velocity decreases with the square of the wave amplitude, which is analogous to the "refractive index" increasing quadratically with the field amplitude in nonlinear optics. This causes self-focusing to occur for a bell-shaped input amplitude profile. The effect manifests itself in the initial reduction of the waist size of the beam before diffraction effects dominate and cause beam spreading. Conversely, self-defocusing is observed at lower frequencies where the phase velocity increases with the square of the wave amplitude, and the beam spreads more than it would have in the linear, diffraction-limited case.

II. EXPERIMENTAL SETUP AND INITIAL OBSERVATIONS

It is important that the generation of subharmonics (possible in the capillary wave regime) be avoided in these experiments. In our earlier experiments we had found that the use of cold, clean water tended to raise the threshold for subharmonic generation.¹ We can expect to raise this threshold even further by having the initial excitation generate a relatively narrow, profiled beam with a maximum on axis,

rather than a plane wave (wide, flat beam) as used in our previous experiments. Consequently we used a narrow (~ 3 cm) paddle with a triangular tip that maximized its immersion in the center. The waves are monitored optically by a Schlieren strobe system to study the propagation of wavefronts, and electrically by a dc resistance probe to study the amplitude profiles during propagation. The experiment was

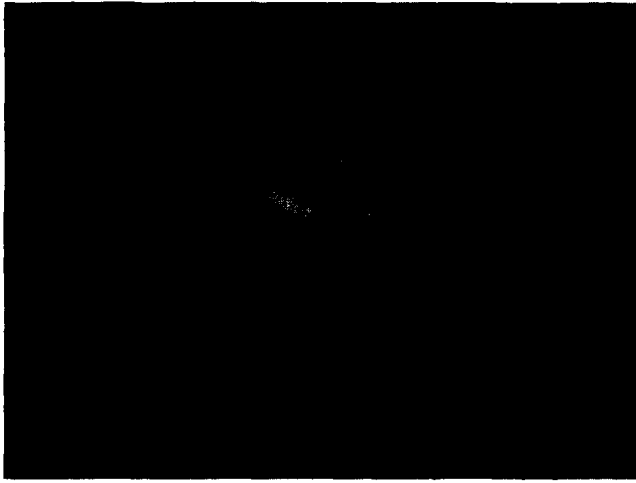


(a)

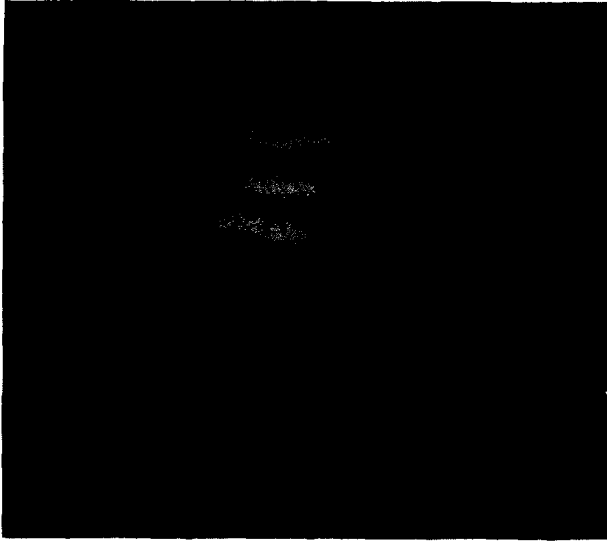


(b)

FIG. 1. Wavefronts on the water surface at 30 Hz (capillary wave regime) (a) for high input amplitudes, showing self-focusing; and (b) for low wave amplitudes. In each case, the paddle is at the top.



(a)



(b)

FIG. 2. Wavefronts on the water surface at 20 Hz (a) for high input amplitudes, showing self-defocusing; and (b) for low wave amplitudes. In each case, the paddle is at the top.

conducted at frequencies between 10 and 70 Hz.

The “frozen” wavefronts of the propagating wave were carefully monitored optically while increasing the wave amplitudes. Self-focusing, characterized by the initial concavity of the wavefronts and reduction of the beam waist size before diffraction effects become dominant, was observed at high amplitudes for the capillary wave regime, and is shown in Fig. 1(a). This figure should be compared with Fig. 1(b) which shows the low-amplitude wavefronts. Conversely, self-defocusing was observed at lower frequencies for high input amplitudes. The resulting increased wavefront convexity and the beam waist size are shown in Fig. 2(a), with Fig. 2(b) again showing the low-level experiment. Care is taken to avoid extremely high amplitudes in the capillary wave regime so as not to exceed the threshold for subharmonic generation.

In passing, it may be noted that Figs. 1(a) and 2(a) show wavefronts similar to those observed in the self-refraction of ion-acoustic waves in plasmas.³

III. THEORY

In a medium in which the phase velocity is quadratically dependent on the wave amplitude, the first-order nonlinear kinematic wave equation may be written as⁴

$$\frac{\partial \psi}{\partial t} + c_0(1 + \beta_3 \psi^2) \frac{\partial \psi}{\partial x} = 0. \quad (1)$$

For extension to higher dimensions, we assume a weak nonlinearity, differentiate (1) with respect to t , use (1) to simplify and replace $\partial^2/\partial x^2$ by $\partial^2/\partial x + \partial^2/\partial y^2$ to get

$$c_0^{-2} \frac{\partial^2 \psi}{\partial t^2} - \frac{\partial^2 \psi}{\partial x^2} - \frac{\partial^2 \psi}{\partial y^2} \approx \beta_3' \frac{\partial^2 \psi^3}{\partial t^2}, \quad \beta_3' = \frac{2}{3} \beta_3 c_0^{-2}. \quad (2)$$

Equation (2) is similar to the wave equation in nonlinear optics where the right-hand side may be identified to be the source term due to the nonlinear polarization of the medium.² The relationship between β_3' and the commonly used nonlinearity parameter $(\partial \omega / \partial a^2) \omega_c$ around a point (ω_c, k_c) of the amplitude-dependent dispersion curve may be found by deriving the latter through substituting $\psi \sim a \cos(\omega t - kx)$ into (1) and equating coefficients at frequency ω . This yields

$$\left. \frac{\partial \omega}{\partial a^2} \right|_{\omega_c} \approx \frac{\beta_3 \omega_c}{4} = \frac{3}{8} \beta_3' \omega_c c_0^2. \quad (3)$$

Even though the wave phenomenon under investigation is dispersive, this is irrelevant to our case of cw propagation. Hence (2) is a sufficiently good model equation if we take c_0 equal to the phase velocity observed in practice.

Making the substitutions

$$\psi(x, y, t) = [a(x, y)e^{-j\phi(x, y)}] e^{j(\omega_c t - k_c x)} + \text{c.c.} \quad (4)$$

(where we have assumed stationarity of the slowly varying envelope) in (2), it may be readily shown⁵ that the following relations are obtained:

$$\begin{aligned} \frac{\partial \phi}{\partial x} + \frac{1}{2k_c} \left(\frac{\partial \phi}{\partial y} \right)^2 + \frac{\gamma}{2k_c} a^2 - \frac{1}{2ak_c} \frac{\partial^2 a}{\partial y^2} &= 0 \\ \gamma = 3\beta_3' \omega_c^2 &= 8 \frac{\omega_c}{c_0^2} \left(\frac{\partial \omega}{\partial a^2} \right), \end{aligned} \quad (5)$$

and

$$\frac{\partial a^2}{\partial x} + \frac{1}{k_c} \frac{\partial}{\partial y} \left(\frac{\partial \phi}{\partial y} a^2 \right) = 0. \quad (6)$$

Note that in (5), the third and fourth terms on the left-hand side represent the contributions of nonlinearity and dispersion, respectively.

A particular solution to the system of Eqs. (5) and (6) in the absence of diffraction has been derived by Akhmanov *et al.*⁶ For the sake of clarity, however, we shall present an approximate solution to (5) and (6) in the presence of nonlinearity and weak diffraction, starting from an initial Gaussian profile. To this end, we look for solutions of (5) and (6) of the form²

$$a^2 = \frac{a_0^2}{h(x)} \exp - \left(\frac{y}{y_0[h(x)]} \right)^2, \quad (7)$$

$$\phi = \frac{1}{2} k_c y^2 p(x) + \tilde{\phi}(x), \quad (8)$$

with

$$\frac{1}{h} \frac{dh}{dx} = p(x), \quad (9)$$

i.e., we look for a solution in terms of a Gaussian beam of width hy_0 having a cylindrical wavefront with a variable radius of curvature $1/p$. The reason for this choice is that a solution of this form, with p and h related as in (9), satisfies the parabolic equations (5) and (6) when $\gamma = 0$, i.e., in the linear diffraction limited case. When $\gamma \neq 0$, (7)–(9) is still a solution of the system (5) and (6) provided $\gamma a^2/2k_c$ is expanded in a power series up to and including terms in y^2 . Thus, (7)–(9) is now an approximate (paraxial) solution to the system valid for $y/y_0 \ll 1$. Substituting (7)–(9) in (5), and equating coefficients of y^2 , we obtain after some algebra, the relation

$$\frac{h''}{h} = \frac{1}{y_0^4 k_c^2 h^4} + \frac{2\gamma' a_0^2}{y_0^2 h^3}, \quad \gamma' = \frac{\gamma}{2k_c^2} = \frac{4}{\omega_c} \left(\frac{\partial \omega}{\partial a^2} \right). \quad (10)$$

Multiplying (10) by $2hh'$, integrating with respect to x , and imposing the initial conditions $h = 1$, $h' = 0$ at $x = 0$, we find

$$h'^2 = \frac{1}{y_0^4 k_c^2} (1 - h^{-2}) - \frac{4a_0^2 \gamma'}{y_0^2} (h^{-1} - 1), \quad (11)$$

where the first term on the right-hand side of (11) is the diffraction term while the second term represents the nonlinear contribution.

In the absence of nonlinearity ($\gamma' = 0$), (11) may be directly integrated to give

$$h^2 = 1 + x^2/y_0^4 k_c^2, \quad (12)$$

which represents beam spreading in the linear, two-dimensional, diffraction-limited case.

In the absence of diffraction, (10) becomes

$$h''/h = 2\gamma' a_0^2/y_0^2 h^3. \quad (13)$$

If $\gamma' < 0$ ($\beta_3 < 0$), i.e., the phase velocity decreases as the square of the wave amplitude, we expect self-focusing. Indeed, under this condition, integration of (13) yields

$$(-2a_0/y_0) \sqrt{-\gamma'} x = \frac{1}{2} \sin 2\theta + \theta, \quad \theta = \cos^{-1} \sqrt{h}, \quad h < 1. \quad (14)$$

If we define the distance to focus as the point where $h = 0$, we notice from (14) that we may have multiple focusing.⁶ For the first point of focus,

$$\theta = -\pi/2; \quad (15)$$

substituting in (14) we obtain

$$x_f \simeq \frac{0.78y_0}{a_0 \sqrt{-\gamma'}} \simeq \frac{0.55w_0}{a_0 \sqrt{-\gamma'}}, \quad (16)$$

where $2w_0$ is the initial width between the $1/e$ points of the amplitude profile (7):

$$y_0^2 = w_0^2/2. \quad (17)$$

Equation (16) agrees essentially with the expression for x_f given by Akhmanov *et al.*⁶ for two-dimensional self-focusing in the absence of diffraction.

For the case of weak diffraction, i.e., when

$$1/k_c y_0 \ll a_0 \sqrt{|\gamma'|}, \quad (18)$$

(11) can be approximately written as

$$h' \simeq \frac{2a_0 \sqrt{-\gamma'}}{y_0} \left(\frac{1-h}{h} \right)^{1/2} \left(1 - \frac{1}{8a_0^2 (-\gamma') y_0^2 k_c^2} \frac{h+1}{h} \right). \quad (19)$$

Integration of (19) yields, after some algebra, the relation

$$-2a_0 \sqrt{-\gamma'} x/y_0 \simeq (\frac{1}{2} \sin 2\theta + \theta) + m(\sin 2\theta + 6\theta),$$

where

$$\begin{aligned} \theta &= \cos^{-1} \sqrt{h}, \\ m &= [16a_0^2 (-\gamma') y_0^2 k_c^2]^{-1} \\ &= [8a_0^2 (-\gamma') w_0^2 k_c^2]^{-1}, \quad h < 1. \end{aligned} \quad (20)$$

To determine the point of focus, we set $h = 0$ so that

$$\theta = -\pi/2, \quad (21)$$

and obtain from (20),

$$x_f \simeq \left(0.55 + \frac{0.42}{a_0^2 (-\gamma') w_0^2 k_c^2} \right) \frac{w_0}{a_0 \sqrt{-\gamma'}}. \quad (22)$$

In the defocusing case, when the phase velocity increases as the square of the wave amplitude ($\gamma' > 0$), the variation of h with distance may be readily shown to be given by

$$2a_0 \sqrt{\gamma'} x/y_0 = \frac{1}{2} \sinh 2\tilde{\theta} + \tilde{\theta}, \quad \tilde{\theta} = \cosh^{-1} \sqrt{h}, \quad h > 1 \quad (23)$$

in the absence of diffraction and by

$$2a_0 \sqrt{\gamma'} x/y_0 = (\frac{1}{2} \sinh 2\tilde{\theta} + \tilde{\theta}) - m(\sinh 2\tilde{\theta} + 6\tilde{\theta}) \quad (24)$$

in the presence of weak diffraction. That the beam spreads much faster now as compared to the linear, diffraction-limited case [predicted by (12)] can be easily established by calculating the distance the wave has to travel for h^2 to double from its initial value in each case. For the linear case, the distance equals $x_d = k_c y_0^2$; while for the nonlinear case, in the absence of diffraction, it equals $x_n = 0.7y_0/a_0 \sqrt{\gamma'}$. Clearly, for weak diffraction (18),

$$x_n \ll x_d. \quad (25)$$

Furthermore, from (23) and (24), it can be easily seen that h increases monotonically with x and tends to infinity as $x \rightarrow \infty$.

IV. EXPERIMENTAL RESULTS

In order to verify the effects of self-focusing and self-defocusing of capillary-gravity waves, the amplitude profiles were monitored at varying distances along the propagation axis (x) by moving the probe parallel to the paddle. The results in the capillary wave regime, at a frequency of 50 Hz, are shown in Figs. 3(a) and 3(b), respectively. The focal distance x_f , taken to be the distance from the paddle to where the waist (defined by the $1/e$ points) is a minimum, is of the order of 4 cm. To compare with the theoretical value, note that (16) and (22) may be rewritten, using (3), (5), and (10), as

$$x_f \simeq \frac{0.7w_0}{a_0} \left(\frac{f_c}{(-\partial \omega / \partial a^2)} \right)^{1/2} \quad (26)$$

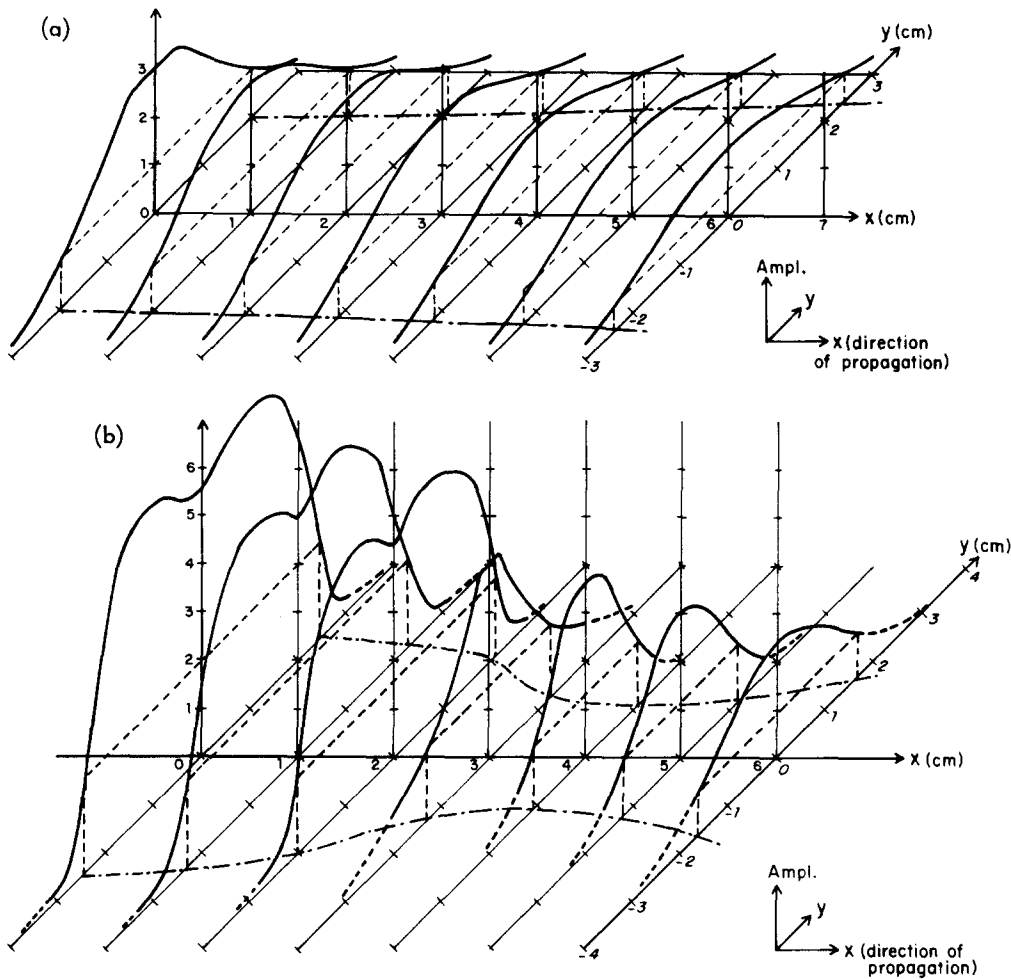


FIG. 3. Measured variation of the amplitude profiles parallel to the paddle, monitored at different points along the direction of propagation at 50 Hz (capillary wave regime) (a) for low input amplitudes; and (b) for high input amplitudes. In each case, dash-dot lines represent the variation in waist size.

and

$$x_f \approx \left(0.7 + \frac{0.8}{a_0^2 w_0^2 k_c^2} \frac{f_c}{(-\partial\omega/\partial a^2)} \right) \left(\frac{f_c}{(-\partial\omega/\partial a^2)} \right)^{1/2} \frac{w_0}{a_0} \quad (27)$$

for the cases of no diffraction and weak diffraction, respectively.

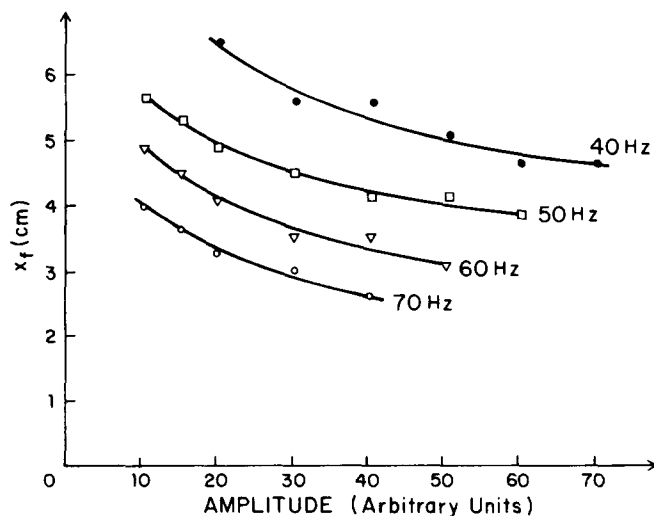


FIG. 4. Measured variation of the focal distance with the initial wave amplitude at different frequencies in the capillary wave regime.

For $f_c = 50$ Hz, $w_0 = 2.5$ cm [from Fig. 3(b)], $a_0 = 1$ mm, and $(\partial\omega/\partial a^2)|_{50 \text{ Hz}} = -2157' / \text{cm}^2 \text{ sec}$ (see Appendix), x_f turns out to be approximately 2.4 cm from (26) or 2.9 cm from (27), in reasonable agreement with the observed value of approximately 4 cm.

The variation of the focal distance with the initial amplitude of the wave profile was also measured at different frequencies. Results are plotted in Fig. 4. Note that x_f decreases with increasing amplitude, in agreement with (26) and (27). Also, for a fixed amplitude, we see that x_f decreases

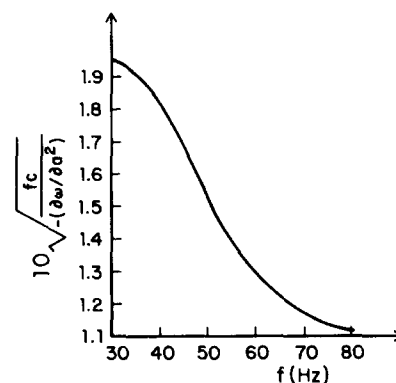


FIG. 5. Theoretical variation of the focal distance $\{ \propto 10 [f_c / (-\partial\omega/\partial a^2)]^{1/2} \}$ with frequency in the capillary wave regime.

with increasing frequency, which, too, is in agreement with the theoretical results that are calculated using (26) and plotted in Fig. 5.

The effects of attenuation on our experiments are relatively small and may be assessed as follows.

Figure 3(a) (which represents the low-level experiments) shows that the attenuation constant at 50 Hz is of the order of 0.06/cm, a value compatible with our earlier findings.¹ If we assume that this value also applies to the high-level experiments, then in Fig. 3(b), we would expect an amplitude reduction of the order of 25% around the point of focus, which is, indeed, seen to be the case. As a rough guess, we would also expect that, to a first order, the *effective* value of a_0 in (16) and (22) would be smaller by the same amount, thereby increasing the effective distance to focus by a proportional fraction. The new expected value of $x_f (= x_{f,\text{eff}})$ under these conditions turns out to be approximately 3.0 or 3.6 cm for the cases of no diffraction or weak diffraction, respectively, which is in better agreement with our observed value of 4 cm.

The results for a 20 Hz frequency are shown in Figs. 6(a) and 6(b), respectively, for small and large amplitudes. For low amplitudes we find that, at a distance of 4 cm from the paddle, the waist is about 1.3 times the initial value. This is in

fair agreement with the theoretical value of approximately 1.15 obtained by the use of (12) with $w_0 = 2$ cm. For high amplitudes, defocusing causes the waist to increase to about 1.6 times its initial value at a distance of 4 cm from the paddle. This appears to be incompatible with values of $\partial\omega/\partial a^2$ predicted by the equation in the Appendix, which in fact predicts self-defocusing only in the regime below ~ 10 Hz. The reason for this is, at present, unknown.

Note that in all experiments the wave amplitude at the center of the paddle shows a small kink for large wave amplitudes [see Figs. 3(b) and 6(b)]. This may be due to a weak attachment of the paddle to the center of the driving loudspeaker.¹ However, it is interesting to note that in spite of this, the effects of self-refraction can be easily observed and can be explained on the basis of our approximate theory.

V. CONCLUSION

In conclusion, we have observed and analyzed self-refraction of capillary-gravity waves in water and found qualitative agreement between theory and experiment. However, defocusing occurred at higher frequencies than predicted from calculations based on theoretical expressions for non-linearity parameters.

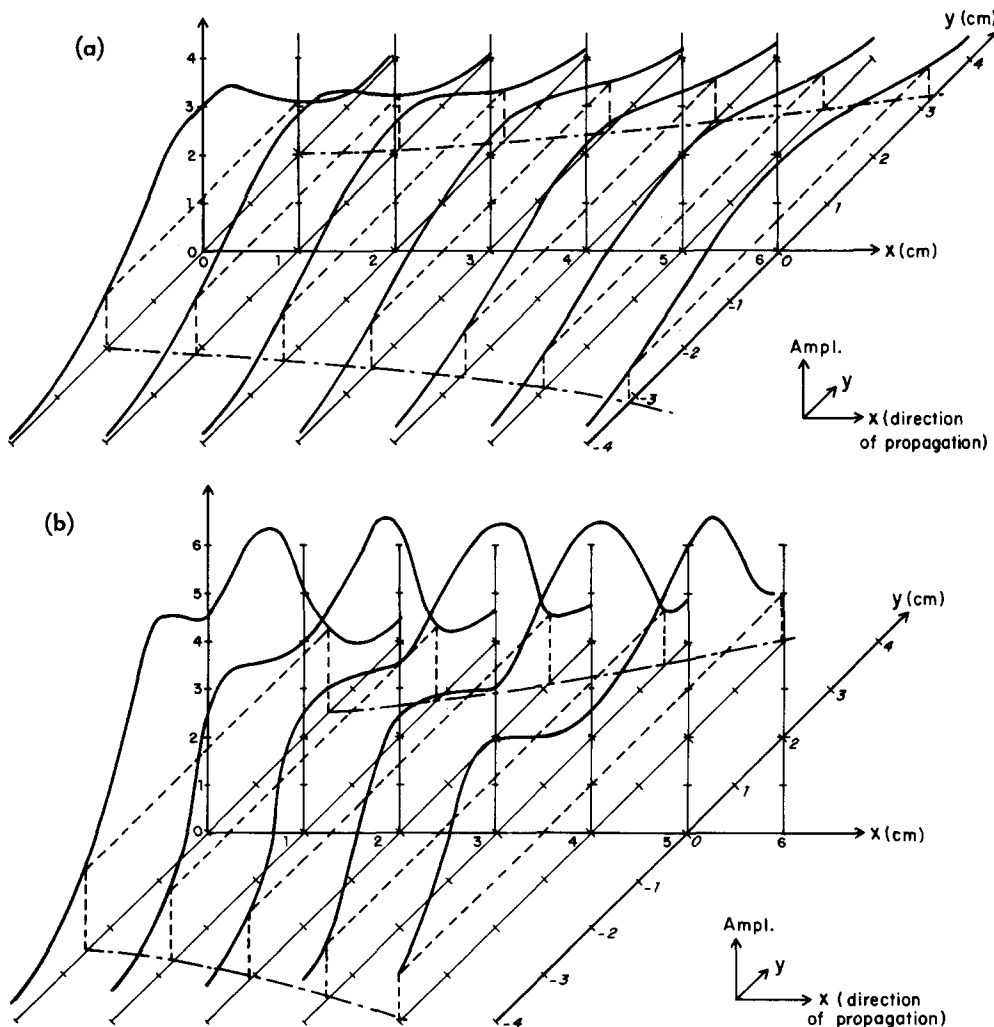


FIG. 6. Measured variation of amplitude profiles parallel to the paddle monitored at different points along the direction of propagation at 20 Hz (a) for low input amplitudes; and (b) for high input amplitudes. In each case, the dash-dot lines represent variation in waist size.

ACKNOWLEDGMENT

The authors acknowledge the support of the National Science Foundation under Grants No. ECS 81-21781 and No. ECS 80-19363.

APPENDIX: DERIVATION OF THE CUBIC NONLINEARITY PARAMETER

In order to evaluate the nonlinear parameters $\partial\omega/\partial a^2$, we must compare the nonlinear Schrödinger equation derived by Karpman⁷ with the results of Djordjevic and Redekopp.⁸ To establish consistency in notation and show necessary relations, we first summarize Karpman's results. Assuming a traveling wave solution of the form

$$\tilde{\Phi}(\bar{r}, t) = \text{Re}[\Phi(\bar{r}, t)], \quad (\text{A1})$$

where

$$\Phi(\bar{r}, t) = \psi(\bar{r}, t)e^{j(k_0 x - \omega_0 t)}, \quad (\text{A2})$$

with

$$\psi(\bar{r}, t) = a(\bar{r}, t)e^{j\phi(\bar{r}, t)}, \quad (\text{A3})$$

and an amplitude-dependent dispersion relation of the form

$$\omega(k, a^2) = \omega_0 + u_0(k - k_0) + \left(\frac{u'_0}{2}\right)(k - k_0)^2 + \left.\frac{\partial\omega}{\partial a^2}\right|_0 a^2, \quad (\text{A4})$$

around (ω_0, k_0) , where

$$u_0 = \left.\frac{\partial\omega}{\partial k}\right|_{k=k_0, a=0}, \quad u'_0 = \left.\frac{\partial^2\omega}{\partial k^2}\right|_{k=k_0, a=0}, \quad (\text{A5})$$

we can obtain, following Karpman, the nonlinear Schrödinger equation for the complex amplitude defined by (A3):

$$j(\psi_t + u_0 \psi_x) + \frac{u'_0}{2} \psi_{xx} + \frac{u_0}{2k_0} \Delta_\perp \psi - \left.\frac{\partial\omega}{\partial a^2}\right|_0 |\psi|^2 \psi = 0, \quad (\text{A6})$$

in which x is the direction of propagation and Δ_\perp the transverse Laplacian. Assuming uniformity in the z direction, transforming to a moving frame of reference given by

$$\xi = x - u_0 t, \quad \tau = t, \quad \eta = y, \quad (\text{A7})$$

and substituting in (A6), we derive

$$j \frac{\partial\psi}{\partial\tau} + \frac{u'_0}{2} \frac{\partial^2\psi}{\partial\xi^2} + \frac{u_0}{2k_0} \frac{\partial^2\psi}{\partial\eta^2} - \left.\frac{\partial\omega}{\partial a^2}\right|_0 |\psi|^2 \psi = 0. \quad (\text{A8})$$

From Djordjevic and Redekopp,⁸ the surface displacement ξ is given by

$$\xi(x, y, t) = \frac{j\omega_0}{g(1 + \tilde{T})} (Ae^{jk_0 x - j\omega_0 t} - A^* e^{-jk_0 x + j\omega_0 t}) \quad (\text{A9})$$

$$= \frac{2\omega_0}{g(1 + \tilde{T})} \text{Re}(jAe^{jk_0 x - j\omega_0 t}), \quad \xi \text{ real}, \quad (\text{A10})$$

where A represents the complex envelope and $\tilde{T} = k_0^2 T/g$, $T = \Gamma/\rho$, Γ being the surface tension of the liquid and g the acceleration due to gravity. Comparing the (A1) and (A2) with (A10),

$$\psi = [2j\omega_0/g(1 + \tilde{T})]A. \quad (\text{A11})$$

The differential equation satisfied by A is given by⁸

$$2j\omega_0 \frac{\partial A}{\partial\tau} + \omega_0 u'_0 \frac{\partial^2 A}{\partial\xi^2} + \frac{\omega_0}{k_0} u_0 \frac{\partial^2 A}{\partial\eta^2} - P|A|^2 A = 0, \quad (\text{A12})$$

where

$$P = \frac{k_0^4}{2} \left(\frac{12\tilde{T}}{1 - 2\tilde{T}} + 8 - \frac{3\tilde{T}}{1 + \tilde{T}} \right), \quad (\text{A13})$$

for the deep-water limit [$kh \rightarrow \infty$, $\Phi_{\xi\xi}^{(1,0)} = 0$ (see, p. 708 of Ref. 8), and $\sigma = \tanh kh \rightarrow 1$]. From (A11) and (A12),

$$j\psi_\tau + \frac{u'_0}{2} \psi_{\xi\xi} + \frac{u_0}{2k_0} \psi_{\eta\eta} - P \frac{g^2(1 + \tilde{T})^2}{8\omega_0^3} |\psi|^2 \psi = 0. \quad (\text{A14})$$

Comparing (A14) and (A8),

$$\left.\frac{\partial\omega}{\partial a^2}\right|_{\omega_0} = \frac{Pg^2(1 + \tilde{T})^2}{8\omega_0^3} = \frac{g^2(1 + \tilde{T})^2}{16\omega_0^3} k_0^4 \left(\frac{8 + \tilde{T} + 2\tilde{T}^2}{(1 - 2\tilde{T})(1 + \tilde{T})} \right). \quad (\text{A15})$$

Note that for capillary waves (i.e., $\tilde{T} \rightarrow \infty$), $\partial\omega/\partial a^2 < 0$ and for gravity waves (i.e., $\tilde{T} \rightarrow 0$), $\partial\omega/\partial a^2 > 0$. The crossover between gravity waves and capillary waves is usually defined as the point $\tilde{T} = \frac{1}{2}$. At this value (~ 10 Hz for 70 dyn/cm surface tension), $\partial\omega/\partial a^2$ changes sign. We find however, that apparently this crossover lies at a higher frequency, because even at 20 Hz we observe apparent self-defocusing and hence must conclude $\partial\omega/\partial a^2 > 0$ at this point.

¹P. P. Banerjee and A. Korpel, *Phys. Fluids* **25**, 1938 (1982).

²O. Svelto, in *Progress in Optics*, edited by E. Wolf (North Holland, Amsterdam, 1974), Vol. XII, p. 3.

³E. Okutsu and Y. Nakamura, *J. Phys. Soc. Jpn.* **51**, 3022 (1982).

⁴G. B. Whitham, *Linear and Nonlinear Waves* (Wiley, New York, 1974), p. 19.

⁵A. K. Ghatak and K. Thyagaragan, *Contemporary Optics* (Plenum, New York, 1978), p. 24.

⁶S. A. Akhmanov, A. P. Sokhorukov, and R. V. Khokhlov, *Sov. Phys. JETP* **24**, 198 (1968).

⁷V. I. Karpman, *Nonlinear Waves in Dispersive Media* (Pergamon, New York, 1975), p. 123.

⁸V. D. Djordjevic and L. G. Redekopp, *J. Fluid Mech.* **79**, 703 (1977).